Step instability of the $In_{0.2}Ga_{0.8}As$ (001) surface during annealing*

Zhang Bi-Chan(张毕禅), Zhou Xun(周 勋), Luo Zi-Jiang(罗子江), Guo Xiang(郭 祥), and Ding Zhao(丁 召)†

Low-Dimensional Semiconductor Structure Laboratory, College of Science, Guizhou University, Guiyang 550025, China

(Received 8 September 2011; revised manuscript received 8 November 2011)

Anisotropic evolution of the step edges on the compressive-strained $In_{0.2}Ga_{0.8}As$/GaAs(001) surface has been investigated by scanning tunneling microscopy (STM). The experiments suggest that step edges are indeed sinuous and protrude somewhere a little way along the $[1\bar{1}0]$ direction, which is different from the classical waviness predicted by the theoretical model. We consider that the monatomic step edges undergo a morphological instability induced by the anisotropic diffusion of adatoms on the terrace during annealing, and we improve a kinetic model of step edge based on the classical Burton–Cabrera–Frank (BCF) model in order to determine the normal velocity of step enlargement. The results show that the normal velocity is proportional to the arc length of the peninsula, which is consistent with the first result of our kinetic model. Additionally, a significant phenomenon is an excess elongation along the $[1\bar{1}0]$ direction at the top of the peninsula with a higher aspect ratio, which is attributed to the restriction of diffusion lengths.

Keywords: InGaAs, step instability, surface diffusion, kinetic model

PACS: 81.05.Ea, 68.55.J–, 68.35.Fx, 81.15.Aa **DOI:** 10.1088/1674-1056/21/4/048101

1. Introduction

InGaAs films with low-indium concentration have been widely applied in the fields of electronic and optoelectronic devices worldwide, due to their high electron mobility. A lattice-mismatched InGaAs film can be prepared on a GaAs (001) buffer by molecular beam epitaxy (MBE), in which way the step edges, in particular on a compressive-strained surface, can easily evolve into sinuous steps due to the fact that the heteroepitaxial layer is inherently unstable.[1] Generally speaking, on an as-grown surface with annealing at a high temperature, the step is never stabilized enough to form a straight step, unless adatoms are frozen on the terrace without surface diffusion at $T = 0$. It therefore appears necessary to understand the origins of step instabilities and, if possible, to suppress them.

For InGaAs compound semiconductor material, extensive research has focused on the transition of two-dimensional (2D) to three-dimensional (3D) growth, which is efficiently caused by promising quantum heterostructures such as InGaAs wells or wires.[2−11] In contrast, the morphology of InGaAs surfaces during growth and annealing has rarely been studied in recent literature. Millunchick *et al.* have given a detailed report on the development of step instability.[12] They observed that the protuberances in the step line are generally elongated in the $[1\bar{1}0]$ direction for all compositions. This anisotropy is attributed to diffusion and attachment, which is expected to be easier along the dimer rows than across the rows.[13]

Based on the general methodology with the versatility of the Burton–Cabrera–Frank (BCF) model,[1,14−16] theoretical treatments of step instability are usually attributed to the nature of a reduction in surface energy, which has been calculated to show that the wavy steps on a vicinal surface are stable rather than straight steps, and that they can lower the surface energy by reducing the size of the stress domains.[17−19] The critical drift velocity of adatoms can induce the instability in a wandering step, and this is calculated through kinetic Monte Carlo simulation.[20−22] There is a crossover of the dominant stress-driven instability from step bunching

*Project supported by the National Natural Science Foundation of China (Grant No. 60866001), the Special Project for Senior Researcher of Guizhou Organization Department (Grnat No. TZJF 2006.10), Doctor Foundation of Guizhou University, the Innovation Fund of Guizhou University (Grant No. 2011008), the Science and Technological Project for Scholar Abroad, Guizhou Province (Grant No. [2007]03), and the Guizhou Science and Technology Foundation (Grant No. J[2007]2176).

†Corresponding author. E-mail: zding@gzu.edu.cn

© 2012 Chinese Physical Society and IOP Publishing Ltd

to step undulation.[23] However, the formation of a sinuous step is rarely treated by a comparison between the kinetic model and experimental results.

The main goal of this paper is to provide a kinetic model of step edge and to give a qualitative conclusion for the step instability of $In_{0.2}Ga_{0.8}As(001)/GaAs$ surfaces. For this purpose we take into account the effect of anisotropic diffusion in order to understand step instability well. An improved linear kinetic model based on the steady-state density of the adatoms of the step edge has been presented. Three kinetic mode results agree well with the step morphology on a 20 ML $In_{0.2}Ga_{0.8}As$ surface. In our experimental results, we observed that unlike the classical waviness described in classical BCF models, a sinuous step has usually undergone several consecutive evolutions during longer annealing. Finally, we give a distribution of the average aspect ratio of peninsulas, which presents a significant increase in aspect ratio when the amplitude of the peninsula exceeds 180 nm. The excess elongation on the top of the peninsula is likely to be caused by the restriction of the surface diffusion of adatoms.

2. Kinetic model of step edge

2.1. Modified BCF model

In epitaxial growth, the vicinal surface generally consists of islands, adatoms and terraces separated by some straight steps, as shown in Fig. 1. We consider a simple process where a flux F of atoms impinges upon the surface and a part of the adatoms will desorb back into vacuum after a certain lifetime τ. But most adatoms are eventually deposited on the terrace and then diffuse on the surface until they attach to a kink of step edge or coalesce with an island. Here, we consider that the motion of adatoms on terraces is impermeable, which crossing the step without solidification are negligibly few.[17] Epitaxial growth on a vicinal surface was treated quantitatively by the versatile BCF model, which shows that the steady-state density of adatoms on the terrace ρ satisfies Eq. (1)

$$D_{\mathrm{s}}\nabla^2\rho - \frac{\rho}{\tau} + F = 0, \tag{1}$$

in which D_{s} is the surface diffusion coefficient, ρ/τ is the desorbed adatoms per unit time and F is the deposition flux rate. Complications due to the step–step interaction and the anisotropy of the surface diffusion and the step strain relaxation are indeed neglected in the BCF model.

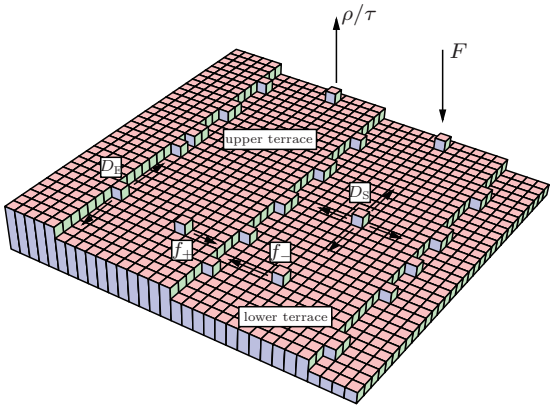


Fig. 1. (colour online) Schematic drawing of a vicinal surface under flux supersaturation during epitaxial growth, showing the terraces, step edges, adatoms, and kinks.

Our purpose in this paper is to attempt to build a kinetic model of step edges in order to further understand the morphological instability during annealing. The BCF model considers that the net density of adatoms on terraces is close to the equilibrium during thin-film growth, and in particular that the kinetics of step attachment are infinitely fast as an ideal step flow model.[1] However, in earlier papers[24,25] and our experience, the attachment rate of adatoms exhibits orientation dependence, which is discussed in detail in Subsection 3.2. In this expression of Eq. (1), the diffusion of adatoms on terraces is isotropic, but at step edges the diffusion coefficient D_{E} should be on a single-line towards two opposed directions. Hence, the BCF theory needs to be modified to reflect the above statement well.

Caflisch *et al.* described a good kinetic model of step edges with time dependence, and their theoretical results agree with kinetic Monte Carlo simulations.[26] Here, we modified the kinetic model based on the steady-state density of the adatoms of the step edge in Eq. (2), which can determine the enlarged velocity of the terrace.

$$D_{\mathrm{E}}\partial_{\mathrm{s}}^2\varphi + f_0 = f_+ + f_- + \frac{\varphi}{\tau}, \tag{2}$$

where D_{E} is the diffusion coefficient of adatoms along the step edge shown in Fig. 1, s is the arc-length variable of the step edge, φ is the density of the adatoms of the step, f_0 is a net flux that adatoms will attach to the kinks, and f_+ and f_- are considered as the net flux of adatoms from the upper terrace and the lower terrace, respectively. Due to our experimental process in annealing conditions, there are no excess atoms to impinge the surface from the solid source and the term F in Eq. (1) should be omitted. The whole annealing process is always under an overpressure and the adatoms desorbing back are relatively small, so the term of φ/τ is also neglected.

2.2. Maximal unstable model

Numerous experiments and theories state that adatoms hopping into kinks from the upper terrace will overcome an excess energy barrier called the Echrlich Schwoebel (ES) potential,[27−29] in which case adatoms attaching to kinks is more likely to be from the lower terrace. Firstly, we suppose a most unstable possibility that appears such that the step edge will become more sinuous with the enlarging of the terrace. An upper terrace and a lower terrace on a vicinal surface descend from left to right as a 'perfect sink' vicinal surface, as shown in Fig. 2, where the waviness $f(y_0)$ is taken to be in the form of a small amplitude cosine curve, and $f(y_1)$ with a larger amplitude is considered as the increased terrace during annealing. Suppose that adatoms will hop into kinks from the upper terrace. Adatoms like to attach with kinks of the A point rather than the B point, due to the shorter hopping distance. Conversely, the contribution from the lower terrace is diminished at the A point and is increased at the B point. For convenience, we define k_+ to be the attachment rate to the kinks from the upper terrace and k_- to be the attachment rate of adatoms from the lower terrace. The above-mentioned attachment rate k_- is in general more effective than k_+. Then the result is obtained that the step edge at the B point will elongate in the direction perpendicular to the step, but at the A point there is no longer an increase. The farther the B point of the step edge moves along the sinking direction, the more the contribution of adatoms from the lower terrace and the less from the upper terrace. It is clear that on this supposition the feedback can lead to a complete instability of step edges.

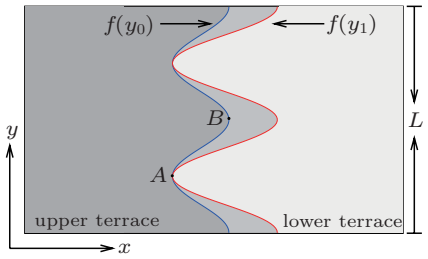


Fig. 2. (colour online) Top view of a vicinal surface including two terraces and two waviness steps (blue and red curves), which reflect the different attachment rates of adatoms to kinks at the A or B point.

To understand step instability during annealing, we suppose a maximally unstable condition in Fig. 2, which is likely consistent with surface diffusion during longer annealing times. We limit the attachment rate so k_+ is reduced to zero, in which case no adatoms arriving from the upper terrace will join the A point. The only possibility is the contribution of adatoms at the A point from the lower terrace. However, it is very hard for adatoms to reach the A point. By contrast, they prefer to attach to a closer step of the B point on the same terrace, due to the short diffusion length, in particular during longer annealing. Hence, the increased ΔT area between $f(y_0)$ and $f(y_1)$ in Eq. (3) appears during the elongation of the terrace edge

$$\Delta T = \int_0^L [f(y_1) - f(y_0)]\,\mathrm{d}y. \tag{3}$$

Here, L is the length of a straight step and can also be considered as the shortest arc length of the step edge.

Almost all of the adatoms, both in the accumulation along the step edge for diffusion and in contributions to the enlarging terrace, are from the surface of the terraces on both sides. Roughly speaking, mass transport to the step edges to ultimately solidify is provided through attachments of adatoms from both terraces due to the conservation of mass of adatoms

$$\int_\Gamma D_\mathrm{E}\partial_s^2\varphi\,\mathrm{d}s + \varphi\frac{\mathrm{d}\Delta T}{\mathrm{d}t} = -\frac{\mathrm{d}}{\mathrm{d}t}\int_{\Omega_+\cup\Omega_-}\rho\,\mathrm{d}A. \tag{4}$$

In addition, the source of net fluxes $f_\pm$ is attributed by all the adatoms on both the upper and lower terraces

$$\int_\Gamma (f_+ + f_-)\,\mathrm{d}s = -\frac{\mathrm{d}}{\mathrm{d}t}\int_{\Omega_+\cup\Omega_-}\rho\,\mathrm{d}A. \tag{5}$$

Considering Eqs. (1), (4), (5), and the result of Eq. (3) (the details are listed in Appendix A), we obtain

$$\int_\Gamma f_0\,\mathrm{d}s = \varphi\left[\frac{\lambda}{2\pi}\sin(\frac{\lambda}{2\pi}L) + L\right]\frac{\mathrm{d}}{\mathrm{d}t}(a_1 - a_0), \tag{6}$$

in which λ is the wavelength of the step, and a_1 and a_0 are the amplitudes of steps $f(y_0)$ and $f(y_1)$, respectively. The net flux f_0 of the adatoms for attaching to kinks is obtained by differentiation with respect to s of both sides of Eq. (6) and we have

$$f_0 = \varphi v_x\frac{\mathrm{d}L}{\mathrm{d}s}, \tag{7}$$

which depends on the velocity v_x in the direction perpendicular to the step

$$v_x = v_0\left[\cos\left(\frac{2\pi}{\lambda}L\right) + 1\right]. \tag{8}$$

It is a function of variable L. Here, the term v_0 is considered to be the growth velocity of the amplitude of step waviness.

In order to express the relative importance of v_x and $\mathrm{d}L/\mathrm{d}s$, we define the terms f_0 and φ in Eq. (7), which are constant during annealing. The term $\mathrm{d}L/\mathrm{d}s$ is indeed an expression of the bending

coefficient of the step edge and its value is between $(0, 1)$. It is clear, for example, that the step is more sinuous when the value becomes almost 0. Conversely, it is more straight when the value is nearly unity. In short, the main results of the above equations can best be summarized as follows.

(i) The faster the normal velocity v_x, the more sinuous it will be, favouring enlarged terraces.

(ii) Along the step edge, the normal velocity v_x can vary as a function of the variable L.

(iii) The degree of step bending has a regular alternation from maximum to minimum along the step.

3. Experimental results and discussion

3.1. Consecutive evolution of the step edge

In our experiment, 20 ML $In_{0.2}Ga_{0.8}As$ films were deposited on the c (4×4) surface of the GaAs (001) buffer layer under As-rich growth conditions in a molecular beam epitaxy (MBE), and the film thickness was verified by the intensity oscillations of the reflection high energy electron diffraction (RHEED) patterns. The growth rates: 0.45 ML/s and 0.36 ML/s for InGaAs and GaAs during the layer-by-layer growth mode, respectively, were also measured by the intensity oscillation of RHEED. Due to the annealing process under a high As flux, the surface was covered by dimer rows of As-terminated reconstructions, all of which were oriented along the $[1\bar{1}0]$ direction on the vicinal terrace. The lattice constant of epitaxial layer ($In_{0.2}Ga_{0.8}As$) is larger than the buffer layer (GaAs), so this heteroepitaxy gives rise to a misfit strain of 1.43% in compression because an In concentration of 20% is deduced from the growth rate of InGaAs and GaAs. At this misfit strain, an InGaAs film 20 ML in height is grown using the layer by layer mode observed on the RHEED image, which is not predicted in the classical SK growth mode. Unlike the straight step of the Si surface, the strained step is indeed unstable during annealing and can be presented through the evolution of step instability. As can be seen, a step line appears to be very sinuous, as marked by a red line in Fig. 3(a). Apparently, all these phenomena with different intensities occur more or less randomly along the step edge during the annealing process. A detailed discussion with some quantitative analysis is made difficult for multiple shapes and random distributions on the strained surface. Therefore, the following analysis is qualitative. Rather, these evolutions do not appear for all of the cusps.

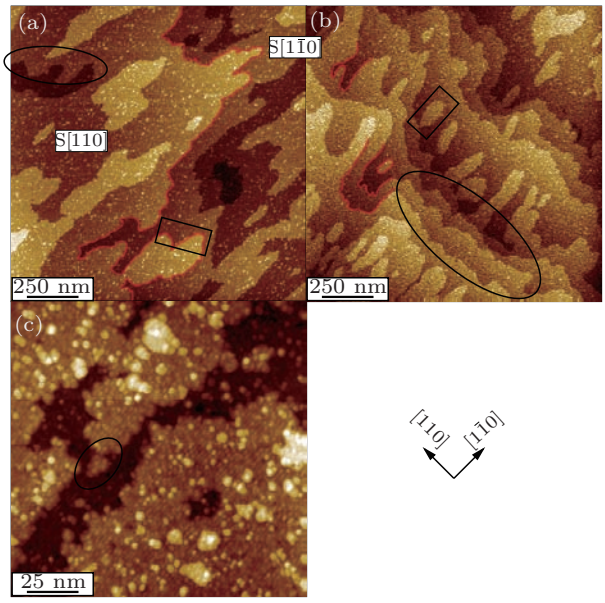


Fig. 3. (colour online) Typical filled state STM images showing the morphological evolution of compressively strained $In_{0.2}Ga_{0.8}As$ films of 20 ML thickness: (a) annealed at T = 460 °C, BEP=1.1 × 10^{-5} Torr (1 Torr=133.3 Pa) for 30 minutes, (b) annealed at T = 470 °C, BEP=0.9 × 10^{-5} Torr for 5 minutes, and (c) annealed at T = 460 °C, BEP=1.1 × 10^{-5} Torr for 10 minutes.

A few of the investigations are summarized now to clarify the evolution of the cusp by some consecutive variations. Firstly, due to the anisotropy of diffusion in the adatoms, the step segments marked 'S $[1\bar{1}0]$' in Fig. 3(a) are all likely to be elongated towards the $[1\bar{1}0]$ direction at the step edge, and a sharp cusp is born between two segments. In addition, the top of the segment is usually very sharp, but a step undulation with a smooth top can also be observed in the rectangle region in Fig. 3(a). Then, the cusps gradually become larger and wider, and some of them penetrate into the terrace along the $[1\bar{1}0]$ direction. Three different cusp developments are shown in the circled region in Fig. 3(a). Furthermore, the top of some of the cusps will be elongated a long distance along the $[1\bar{1}0]$ direction and form a 'bay' shape in the terrace edge, as usually observed experimentally. If the elongation is not in the same direction, the corresponding distance will appear shorter.

Certainly, the 'bay' shape is not the ultimate variation. A two-dimensional (2D) pit is formed inside the terrace through the closing of the neck of the cusps, and this is filled by a tiny island. This evolution is luckily observed in the atomic level image shown in the circled region in Fig. 3(c). However, forming a

2D pit is not the only evolution. Some cusps are allowed to keep penetrating into the depth of the terrace, especially along the [1$\bar{1}$0] direction. Two small branches, which are marked by a red line in Fig. 3(b), have formed in the top of the cusp, and the protrudent island will be encircled completely by both branches. In addition, a bilayer cusp, at which a larger cusp penetrates into a terrace of double layers, is also observed and a new island in the center of the cusp is detached from the neighbouring step. The third evolution of cusps is where the neck of a peninsula is cut off to form a new 2D island, shown in the rectangular region of Fig. 3(b), in which case two cusps penetrate into the same terrace toward the opposed directions. Continuous cutting will cause more and more 2D islands, which will detach from the step resulting in a taller stacked terrace with multi-monolayer narrow steps, as shown in the circled region in Fig. 3(b). Finally, a number of detachments of 2D islands will reduce the coverage of the terraces and eventually lead to the roughness of the well vicinal surface. The evolutions described above show that steps may initially undergo a relaxation of surface energy during annealing. In theory, the energy of the surface steps is negative for compressive strain surface.[12,30] Hence, it is reasonable to conclude that sufficient sinuous steps are more in favour of the stability than wavy steps or straight steps, due to the lengthening of the step edge that lowers the initial value of the energy of the whole surface.

3.2. Anisotropic diffusions

In the case of $In_{0.2}Ga_{0.8}As$, the surface diffusion is highly anisotropic, which remarkably influences the morphology of the steps. This behaviour is mainly the consequence of a preferential attachment of adatoms along the [1$\bar{1}$0] direction. A qualitative conclusion can be drawn on the surface of $In_{0.2}Ga_{0.8}As$ reconstruction, which is separated by dimer rows in the [110] direction. Along the [1$\bar{1}$0] direction, adatoms can easily run along the trench between the dimer rows. However, the mobility along the [110] direction requires that the adatoms have more kinetic energy to climb up the dimer row. In any case, the considerable differences between the energy barriers in the dimer rows and in the trench should lead to a strong anisotropy of surface diffusion. The anisotropy is not surprising. Apart from the ternary compound semiconductors, the diffusion of Si adatoms on Si (001) is of the order of 1000 times faster along the surface dimer rows than across them.[31] In conclusion, the result is that adatoms are expected to prefer to attach to kinks and form a peninsular step along the [1$\bar{1}$0] direction. Hence, the morphological evolution of step edges where the normal velocity of the enlarging step is obviously faster than that of the parallel step will appear .

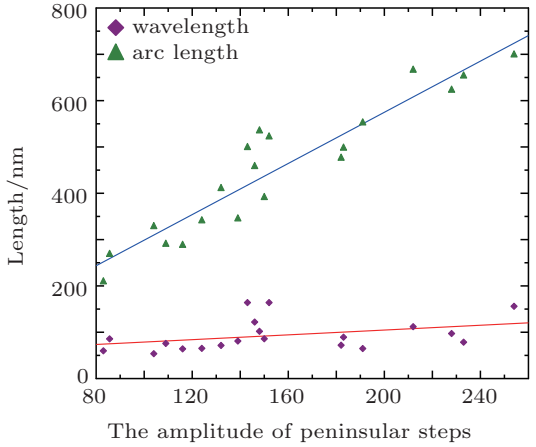


Fig. 4. (colour online) The distribution of wavelength and arc length as functions of the amplitude of the peninsula during the annealing of 20 ML $In_{0.2}Ga_{0.8}As$ films. The red and blue lines are the general trends of wavelength and arc length, respectively.

Figure 4 shows the distribution of wavelength and arc length as functions of the amplitude of the peninsular step. All the step morphology lengths are measured at at least five different positions on the same scale STM images employing the polygon measuring tool in the scanning probe image processor software (SPIP). It is obvious that the wavelengths are just increased slightly, but the arc lengths rise greatly with the increasing amplitude of the peninsula. Here, the amplitude of the peninsula is considered as a distance of the normal mobility of the step edge at certain times during annealing. And the wavelength and arc length are consistent with the step shape in Fig. 2. As discussed above, due to a faster normal velocity, more adatoms are likely to move and attach to steps along the [1$\bar{1}$0] direction, which results in a longer arc length s of the edge of the peninsula. On account of the shorter diffusion length, adatoms on the lower terraces are very hard to move the similar A point (in Fig. 2) to accumulate together for increasing the wavelength. On the contrary, when they pass by the similar B point, most prefer to be close to the side of the convex arc. This behaviour of the attachments leads to a different normal velocity of step enlargement as a function of position at the step edge. The faster normal velocity and slower normal velocity could cause a regular alternation by one crest and one trough, re-

spectively. The above features agree well with the three results of our kinetic model.

3.3. The aspect ratio of the peninsula

In order to quantify step instability, we measured the average aspect ratio (L/W), corresponding to the length in the [1$\bar{1}$0] direction and the width in the [110] direction. A typical result for the average aspect ratio as a function of the amplitude of the peninsula is shown in Fig. 5. As can be seen, when the amplitude is less than 180 nm, the aspect ratio appears to have saturated, which shows that it is limited in the range from 0.5 to 2. Interestingly, the aspect ratio has a broad distribution in the range from 1.6 to 4.6, with the amplitude increasing over 180 nm. To more easily understand the step morphology, we give two figures with different aspect ratios at the top of Fig. 5. The aspect ratios of 5(a) is approximately 1.3, and that of 5(b) is close to 2.5. A significant phenomenon at the (a) peninsula is that the top protrudes somewhat along the [1$\bar{1}$0] direction, and at the (b) peninsulas the top evolves into a sharp protrusion with a higher aspect ratio, which is consistent with the distribution of aspect ratio in Fig. 5. It seems that the

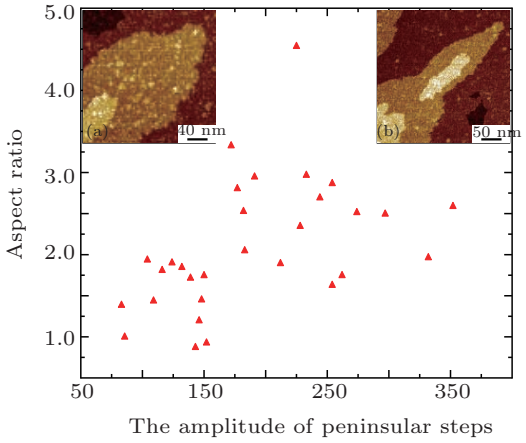


Fig. 5. (colour online) The distribution of aspect ratio as a function of the amplitude of the peninsular step during the annealing of 20 ML $In_{0.2}Ga_{0.8}As$ films: (a) a typical morphology of the peninsula with a smaller curvature, and (b) a sharp protrusion with a bigger curvature at the top of the peninsula.

protrusion may undergo a shape restriction, which could result in the enlargement of the step easily along the [1$\bar{1}$0] direction and hardly along the [110] direction on a strained vicinal surface.

Considering that adatoms randomly hop from one site to another on terraces in order to reach a local minimal energy, the probability of such an adatom hopping process is usually given by the Arrhenius behaviour in Eq. (9)

$$\Gamma(T) = \Gamma_0 \exp \frac{-E_B}{k_B T}, \tag{9}$$

where Γ is the hopping rate as a function of temperature T, and E_B is the activation energy for adatom hopping. The prefactor Γ_0 is related to the hopping rate without thermal activation. Apparently for a certain annealing temperature, the hopping rate should be determined by a restricted frequency of local minimal energy, and it can also be considered that in spite of the faster velocity in the [1$\bar{1}$0] direction, adatoms do not have enough energy to provide a large amount of activation energy to move a further length along this direction due to the conservation of energy. Hence, adatoms should have certain diffusion lengths for a fixed annealing temperature.

At the beginning of annealing, the density of adatoms on the terraces is so high that the step can be entirely enlarged toward the [1$\bar{1}$0] direction for our sample. This behaviour cannot cause significant changes in the morphology of the peninsula. Accordingly, the aspect ratio of the peninsula is maintained in a small range. When the amplitude of the peninsula gradually increases over a critical length, i.e. 180 nm, it is hard for adatoms to arrive at the A point in Fig. 2, but they can easily reach and attach to the B point, which is still in the range of diffusion length while A point out. In fact, this phenomenon is very common in our experiment during longer annealing. The result is that numerous adatoms accumulate together and attach to the step, and then solidify to elongate the top peninsula. On the contrary, the wavelength increases less. This qualitative conclusion can be considered as the cause of the rapid rise in aspect ratio when the amplitude of the peninsula exceeds a certain length.

4. Conclusion

In our experimental results, we observed that unlike the waviness described in classical theoretical models, the step is indeed sinuous and will usually undergo several consecutive evolutions and eventually stabilize. In order to further understand the mechanism of step instability, we give a kinetic model modified from the versatile BCF model and work out three results about the normal velocity, which are consistent with the experimental phenomenon on the compressively strained $In_{0.2}Ga_{0.8}As/GaAs$ (001) surface. Our results from the STM images show that somewhere the step edges are elongated by a longer distance in

the $[1\bar{1}0]$ direction. We consider that this anisotropy is caused by the restriction of the diffusion lengths of the adatoms on the terraces, and give a convincing explanation in the kinetic model. Accordingly, we give a measurement of the distributions of the arc lengths and aspect ratios as functions of amplitude. In particular, the average aspect ratio of the peninsula has a rapid increase when the amplitude reaches a certain length.

Appendix A

We now give the exact expressions of the functions involved in Eq. (3)

$$\begin{aligned}\Delta T &= \int_0^L [f(y_1) - f(y_0)]\,\mathrm{d}y \\ &= \int_0^L \left[a_1 \cos\left(\frac{2\pi}{\lambda}y\right) + a_1 \right. \\ &\quad \left. - a_0 \cos\left(\frac{2\pi}{\lambda}y\right) - a_0\right]\mathrm{d}y \\ &= (a_1 - a_0)\left[\frac{\lambda}{2\pi}\sin\left(\frac{2\pi}{\lambda}L\right) + L\right].\end{aligned}$$

Combining Eqs. (2), (4), and (5), we obtain

$$\begin{aligned}\int_\Gamma f_0\,\mathrm{d}s &= \varphi\frac{\mathrm{d}\Delta T}{\mathrm{d}t} \\ &= \varphi\frac{\mathrm{d}}{\mathrm{d}t}\left[(a_1 - a_0)\left(\frac{\lambda}{2\pi}\sin\left(\frac{2\pi}{\lambda}L\right) + L\right)\right].\end{aligned}$$

By the differentiation of s for both sides of the above equation with respect to s, we have

$$\begin{aligned}f_0 &= \varphi v_0\frac{\mathrm{d}}{\mathrm{d}s}\left[\frac{\lambda}{2\pi}\sin\left(\frac{2\pi}{\lambda}L\right) + L\right] \\ &= \varphi\left[v_0\left(\cos\left(\frac{2\pi}{\lambda}L\right) + 1\right)\right]\frac{\mathrm{d}L}{\mathrm{d}s} \\ &= \varphi v_x\frac{\mathrm{d}L}{\mathrm{d}s}.\end{aligned}$$

References

[1] Bales G S and Zangwill A 1990 *Phys. Rev.* B **41** 5500

[2] Zhou G Y, Chen Y H, Yu J L, Zhou X L, Ye X L, Jin P and Wang Z G 2011 *Appl. Phys. Lett.* **98** 071914

[3] Riotte M, Fohtung E, Grigoriev D, Minkevich A A, Slobodskyy T, Schmidbauer M, Metzger T H, Hu D Z, Schaadt D M and Baumbach T 2010 *Appl. Phys. Lett.* **96** 083102

[4] Mazur Y I, Ma W Q, Wang X, Wang Z M, Salamo G J, Xiaoa M, Mishima T D and Johnson M B 2003 *Appl. Phys. Lett.* **83** 987

[5] Tersoff K and Tromp R M 1993 *Phys. Rev. Lett.* **70** 18

[6] Xu J B, Zhang H Y, Fu X J, Guo T Y and Huang J 2010 *Chin. Phys.* B **19** 037302

[7] Wang M, Gu Y X, Ji H M, Yang T and Wang Z G 2011 *Chin. Phys.* B **20** 077301

[8] Guan B L, Ren X J, Li C, Li S, Shi G Z and Guo X 2011 *Chin. Phys.* B **20** 094206

[9] Gao H L, Li D L, Zhou W Z, Shang L Y, Wang B Q, Zhu Z P and Zeng Y P 2007 *Acta Phys. Sin.* **56** 4955 (in Chinese)

[10] Wang B R, Sun Z, Xu Z Y, Sun B Q, Ji Y, Wang Z M and Salamo G J 2008 *Acta Phys. Sin.* **57** 1908 (in Chinese)

[11] Yang X J, Wang Q, Ma W Q and Chen L H 2007 *Acta Phys. Sin.* **56** 5429 (in Chinese)

[12] Riposan A, Martin G K M and Millunchick J M 2003 *Appl. Phys. Lett.* **83** 22

[13] Shitara T, Zhang J, Neave J H and Joyce B A 1992 *J. Appl. Phys.* **71** 4299

[14] Burton W K, Cabrera N and Frank F C 1951 *Philos. Trans. R. Soc. London* Ser. A **243** 299

[15] Ratsch C, Nelson M D and Zangwll A 1994 *Phys. Rev.* B **50** 14489

[16] Frisch T and Verga A 2005 *Phys. Rev. Lett.* **94** 226102

[17] Tersoff J and Pehlke E 1992 *Phys. Rev. Lett.* **68** 816

[18] Kaganer V M and Ploog K H 2001 *Solid State Commun.* **117** 337

[19] Xie Y H, Gilmer G H and Roland C 1994 *Phys. Rev. Lett.* **73** 3006

[20] Sato M, Uwaha M and Saito Y 2000 *Phys. Rev.* B **62** 12

[21] Grandjean N and Massies J 1993 *J. Cryst. Growth* **134** 51

[22] Saito Y and Uwaha M 1994 *Phys. Rev.* B **49** 10677

[23] Leonard F and Tersoff J 2003 *Appl. Phys. Lett.* **83** 72

[24] Fink H W and Ehrlich G 1986 *Surf. Sci.* **173** 128

[25] Ysuchiya M, Petroff P M and Coldren L A 1989 *Appl. Phys. Lett.* **54** 1690

[26] Caflisch R E, Weinan E, Gyure M F and Ratsch C 1999 *Phys. Rev.* E **59** 6879

[27] Ehrlich G and Hudda F G 1966 *J. Chem. Phys.* **44** 1039

[28] Schwoebel R L and Shipsey E J 1966 *J. Appl. Phys.* **37** 3682

[29] Steigerwald D A, Jacob I and Egelhoff W F 1988 *Surf. Sci.* **202** 472

[30] Kaganer V M and Ploog K H 2001 *Phys. Rev.* B **64** 205301

[31] Mo Y W, Kleiner J, Webb M B and Lagally M G 1991 *Appl. Phys. Lett.* **66** 1998